The analysis of dissolved inorganic carbon in liquid using a microfluidic conductivity sensor with membrane separation of CO_2.

M. Tweedie[1], D. Sun[2], D.R. Gajula[3], B. Ward[4], P.D. Maguire[1].

Abstract.
Autonomous and continuous analysis of ocean chemistry, in particular dissolved inorganic carbon (DIC) concentration profiles with depth, are of great significance with regard to ocean acidification and climate change. However, the development of suitable miniature in-situ analysis systems is hampered by the size, cost and power requirements of traditional optical analysis instrumentation. Here we report a low-cost alternative approach based on CO_2 separation and conductance measurement in microfluidic cells that could pave the way to integrated lab on chip systems for long-term ocean float deployment. Conductimetric determination of dissolved inorganic carbon concentration, in the seawater range of 1000 – 3000 μmol kg^{-1}, has been achieved using a microfluidic thin film electrode conductivity cell and a membrane-based gas exchange cell. After transfer across the membrane, the eluted CO_2 reacted in a NaOH carrier, was drawn through a conductivity cell with a < 1 μL interelectrode volume, where the change in impedance versus time was measured. Precision values, obtained from relative standard deviation, were ~ 0.2 % for peak height measurements over extended time periods. This compares favourably with precision values of ~ 0.25 % obtained using a large C4D electrophoresis headstage with similar measurement volume. The required sample and reagent volumes amounted to ~ 500 μL in total due to the incorporation of a planar membrane into a small volume exchange cell. This compares very favourably with previous attempts at conductivity based DIC analysis where total volumes between 5000 μL and 10000 μL were required. The use of long membrane tubes and macroscopic wire electrodes is avoided by incorporating a planar membrane (PDMS) between sample and exchange cell and by sputter deposition of Ti/Au multilayer electrode patterns directly onto a patterned thermoplastic (PMMA) manifold. Future performance improvement will require addressing membrane chemical and mechanical stability as well as further volume reduction and component integration into a single manifold.

✉ m.tweedie@ulster.ac.uk, pd.maguire@ulster.ac.uk

1 Nanotechnology and Integrated BioEngineering Centre (NIBEC), Ulster University, Jordanstown, Newtownabbey, BT37 0QB, UK.
2 School of Mechanical and Aerospace Engineering, Queen's University, Belfast, BT9 5AH, UK.
3 Clemson University, Dept. of Electrical and Computer Engineering, Clemson SC 29634, USA
4 AirSea Laboratory, Ryan Institute and School of Physics, National University of Ireland, Galway

Keywords Conductivity, Dissolved Inorganic Carbon, CO_2, Ocean Chemistry, Microfluidics, PDMS membrane

1 Introduction.

Atmospheric carbon dioxide concentration has increased significantly due to human activity and is a primary contributor to global warming. The ocean is a major sink for anthropogenic CO_2, mitigating the effects of atmospheric emissions with the CO_2 uptake causing changes to ocean chemistry.[1] However, the ability of the oceans to continue absorption at historic levels is doubtful and the impact of the resultant climate change may be much more serious than predicted. While the importance of ocean chemistry is recognised, our ability to measure ocean variables with sufficient resolution and accuracy is severely restricted due to a lack of analysis systems capable of low cost and widespread deployment.

The ocean CO_2 system is typically characterized by measuring two or more of the four canonical "master variables": partial pressure of CO_2 (pCO_2), pH, total dissolved inorganic carbon (DIC) and total alkalinity (A_T).[2] At present, CO_2 measurements are mainly carried out at the surface, using large volume sensors on research ships.[3] To fully meet the

data needs of climate models, depth profile measurements are required continuously from across the world's oceans. As both pCO_2 and pH are very sensitive to temperature and pressure, they must be measured in-situ and while microfluidic miniaturisation approaches for in-situ surface measurements are currently being developed, autonomous measurements of DIC or A_T would be preferred.[4,5] Given the technical challenges, however, such approaches have yet to be realised.[6] Several methods of Total CO_2 (TCO_2 or DIC) determination have been reported, e.g. gas chromatography[7], membrane inlet mass spectroscopy[8-11], non-dispersive IR[12-15] and spectrophotometry[16-20]. These are large systems and unfortunately do not offer an obvious route to miniaturisation. Recently a compact LED-based spectrophotometric instrument for in-situ measurement has been reported, capable of achieving DIC precision of ±2.5 μmol kg^{-1} with a 700 μL sample cell and total sample and reagent volumes of 9000 μL per sample.[21]

Coulometry is the recommended standard operating procedure for bench DIC determination[22]. The flow injection method of Hall and Aller[23] however, is based on a conductimetric technique and offers greater opportunity for miniaturisation. The standard concentration of total dissolved CO_2 in seawater at sea level is around 1900 μmol kg^{-1}, rising to > 2400 μmol kg^{-1} at depth[19], assuming current values of pH (~ 8.2) and atmospheric CO_2 content (400 ppm)[24]. At these pH values, dissolved CO_2 exists mainly as the bicarbonate, HCO_3^-, and carbonate ions, CO_3^{2-}. The addition of excess acid to reduce the pH to ≤ 4.5, releases DIC as gaseous CO_2 into the aqueous phase which can then be separated by a gas exchange membrane and collected in a receiving solution, typically NaOH (~ 7 – 10 mM). Provided the pH of this solution is sufficient the total added $CO_2^{aq.}$ is converted to CO_3^{2-} through reaction with OH^- and due to the lower mobility of the former, the fluid conductivity is reduced in direct proportion to the added CO_2 concentration. Fluid conductance/impedance techniques are rarely considered for high resolution chemical analysis as accuracy and precision are generally poorer than with colorimetric or optical techniques. This is exacerbated with small sample volumes when deployed in a microfluidic structure. The full ocean DIC concentration range varies with depth from 1700 μmol kg^{-1} to 2800 μmol kg^{-1} and, over this range, a linear decrease in receiver solution conductivity from 125 – 96 mS m^{-1} (>15%) is expected. The reference receiver solution (NaOH, 7 – 10 mM range) conductivity is ~170 mS m^{-1} [25] to 220 mS m^{-1} [23], depending on concentration chosen. The use of conductimetric techniques for determining DIC concentration has been reported.[25,26] Sayles and Eck used a ~150 μL conductivity cell containing Pt wires and a 1000 μL sample cell, with a silicone inner tube containing NaOH which acts as the membrane receiving cell (330 μL).[25] The analysis time per sample was ~1 hr and required sample and reagent volumes (acid, NaOH) of 2500 μL and 8500 μL respectively. In laboratory and field tests they obtained precision values of ±2.2 μmol kg^{-1} and ±3.6 μmol kg^{-1}, equivalent to relative standard deviations (RSD) of ±0.11% and ±0.18% respectively. For laboratory DIC calibration measurements using standard operating procedures (coulometric), cited precision values are typically ±1.5 – ±2.0 μmol kg^{-1}.[22] Plant et al. also used a conductimetric approach to detect ammonium in marine environments.[27] The sample and receiving channels (100 μL / 50 μL) were formed in two thermoplastic blocks which sandwiched a thin PTFE membrane and the conductivity cell (50 μL) comprised two macroscopic plates. A detection limit of 0.2 μM was achieved with minimum error levels of 2.5% (above 3 μM). The accuracy was limited by the transfer of ions across the semi-porous PTFE membrane. The analysis time was ~7 min and required sample and reagent volumes of 1650 μL and 3800 μL respectively. Other conductimetric cell designs include concentric metal tubes[28] and contactless arrangements involving insulated wire pairs[29] or a capillary electrophoresis (C4D) headstage.[26] In the latter work diffusion time, membrane type and surface area to cell volume was investigated for sample volumes up to 300 μL. Although the headstage unit was relatively large, each measurement point required a very small volume of liquid (< 5 μL) and with signal averaging, a precision of ~0.1% was achieved.

An ideal deployment approach for sub-surface and depth profile DIC measurements would be to integrate a miniaturised DIC sensor onto an ocean profiling float.[30] DIC insensitivity to pressure and temperature would allow for sample collection at different depths for subsequent analysis elsewhere. The Argo network[31] currently consists of > 3000 globally distributed autonomous ocean profile floats, providing continuous depth profiling of salinity and temperature, on a 10-day cycle. Each float drifts in the open ocean for up to 3 years and is programmed to profile the upper 2 km of ocean every 7-10 days with the data then transmitted to satellite. This float array infrastructure is eagerly awaiting new autonomous chemical sensor technology but imposes severe constraints on device footprint, volume, power consumption and long-term environmental stability under high pressure cycling (up to 200 atm). These constraints represent a significant challenge for microfluidics fabrication and testing. Typically, Argo floats, with diameters in the range 120 mm – 170 mm, offer a sensor payload capability of about 1.5 Kg, while currently available sensors vary in volume from about 0.2 L to over 3 L. With regard to volume and weight constraints alone, future DIC sensors would need to operate long term with total reagent volumes less than 1 L. At 100 samples per profile and 100 – 200 profiles over the life of the float, reagent limits per sample are therefore < 100 μL and when considering the requirements of sample flushing between measurements, this limit may be lowered considerably. The reagent limit in turn determines the maximum sample (V_S) and receiver cell (V_R) volumes and the conductivity

measurement cell volume is then given by V_R/N where N is the desired number of measurements per elution profile. Overall, the requirement for sub-microlitre cells represents a significant challenge for both fabrication and detection accuracy and precision. In addition, for the long-term and harsh environment operation, robust chemically resilient device bonding is essential with additional features, e.g. multiple layers, mixed materials and multi-channel structures, not normally considered in mainstream microfluidics which is focussed primarily on biomedical applications. Recently we demonstrated long-term PDMS membrane bonding within a thermoplastic manifold[32] as well high pressure resilient thermoplastic bonding for multi-layer and multi-channel devices.[33] In this work, we investigate direct contact conductivity cells with active volumes between 0.5 µL and 2.0 µL for DIC detection in the seawater range 1900 – 2400 µmol Kg^{-1}. For these volumes, the use of macroscopic wires or plates as electrodes is not feasible and instead, we developed a thin film metallisation process onto PMMA using a sputtered thin film of gold (< 200 nm) on top of a 10 nm adhesion promoting inter-layer of sputtered Ti.

3 Experimental

3.1 Conductivity Cell

Metal electrodes were fabricated by RF sputtering of a Ti adhesion layer (< 10 nm), followed by DC magnetron sputtering of an Au layer (~200 nm) through a shadow mask onto flat PMMA substrates to form the electrode pattern. This was then bonded to a second PMMA manifold, wherein the fluid channel had been formed, using $CHCl_3$ solvent vapour assisted thermocompression bonding at 80°C in vacuum.[33] Electrode integrity was tested for resilience against NaOH (9 mM, pH 12) corrosion over several weeks. The electrode cell construction is illustrated in figure 1. Microfluidic channels were milled with an equal height and width of 0.5 mm and the electrode gap was varied from 0.25 mm to 2 mm, giving an active measurement volume range of 0.5 µL to 2.0 µL. The cells were completed with the attachment of Nanoport fluidic connections using epoxy and sealed with silicone, for subsequent immersion in a temperature-controlled (± 0.05 °C) water bath. A Solartron SI 1260 Impedance/Gain-phase analyser (100 mV AC rms, 0V DC) was used to measure the fluid impedance real and imaginary terms at a data acquisition rate of 0.2 Hz. The excitation frequency (≥ 50 kHz) was chosen to minimise the phase angle and the real component, Z', was used as the measure of resistance. Cell calibration was undertaken with standard KCl solutions (Hanna Instruments). Two solutions with a conductivity difference of 1% (139.9 mS m^{-1} and 141.3 mS m^{-1}) were used for repetitively switched sampling. An Elveflow AF1 P1600 pump, with manually operated valves, was used to pressurise a bottle of each solution in turn and the solution bottles and sensor cell were held in a Heraeus oven at 27.5 °C. For comparison, a contactless capillary electrophoresis headstage and controller (eDAQ ET125/ER225 C4D) was used.[26] The fluid conductivity is determined within a capillary tube using external electrodes driven at high frequency (1.2 MHz) and voltage (200V), acquiring data points at a rate of 1 Hz. The active measurement volume between electrodes was ~ 2 µL.

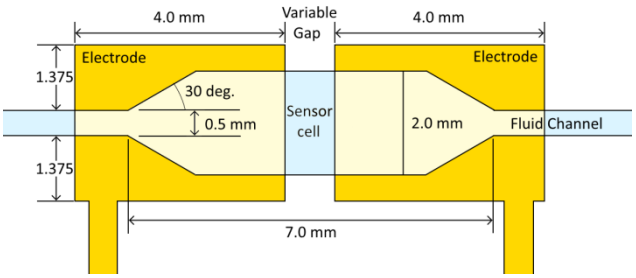

Fig. 1 Electrode pair and sensor cell schematic.

3.2 Membrane Exchange Cell

To operate at reduced volumes, the use of silicone tubes as previously reported is not practical.[17,19-21,26] The membrane exchange cell consists therefore of two PMMA substrates with patterned sample and receiving chambers along with associated microfluidic channels and fluid connectors, separated by a thin membrane sheet. Recently we investigated a range of membrane sheet materials to determine optimum CO_2 exchange versus unwanted ion conductivity and from this it was clear that PDMS performance is far superior to other materials,[32] especially compared to PTFE membranes that have been previously reported.[27] A series of chambers of 1 mm square cross-section and variable length up to 300 mm were fabricated on separate substrates with a 50 µm PDMS film membrane (Goodfellow Cambridge Ltd.). Under static conditions, CO_2 loaded solutions were prepared by mixing preset amounts of 0.1 M $NaHCO_3$ (Sigma Aldrich UK) with degassed DI water to which 5% v/v of 0.1 M HCl was added

either in a sealed vessel, or in a syringe. After 20 - 25 min reaction time, the sample was injected at the diffusion test cell input. For initial diffusion cell comparisons and calibration testing, the receiver (NaOH) chamber was purged with fresh solution using a programmable syringe pump (Aladdin) before the CO_2 sample was added to the sample chamber. A diffusion time of 20 min allowed sufficient exchange of CO_2 from sample to receiver chamber across the membrane. The CO_2-loaded NaOH solution was then pumped through the Au and C4D sensor cells, for impedance measurement, and the cycle repeated as desired. Calibrations were performed for 0.5 – 3.0 mM TCO_2 using a ~200 µL receiving chamber and a total sample volume of 1 mL**.**

For continuous flow measurement, HCl acid is injected into the $NaHCO_3$ flow stream, rather than by pre-mixing. For this we used an asymmetric Y-junction reagent meter, fabricated in-house by CO_2 laser etching of PMMA and sealed by solvent ($CHCl_3$) vapour assisted bonding.[33] A sample to acid meter ratio of ~ 6:1 was achieved. Exchange volumes were 100 µL, with NaOH reagent volumes for the elution curve of 350 – 600 µL, depending on flow rate. Cetoni NeMeSys syringe pumps, with QMix control software, were used to draw fluid through both sides of the gas exchange cell in sequence. The TCO_2 solution was drawn through at a fixed rate (7.5 – 8.5 µL s^{-1}), followed by 15 min diffusion. NaOH was then drawn through at a fixed rate 1.5 - 1.7 µL s^{-1}. Each elution peak was therefore at least 200 s. A small number of samples were drawn through at 12 µL s^{-1} to evaluate the impact of high flow rates. A temperature stabilised water bath, using an NE4-D/CT Clifton digital temperature-controlled heater and stirrer, in combination with a DC1-300 Clifton chiller, was used to compensate for long term thermal drifts. The stated temperature sensitivity, after stabilisation, is ± 0.05°C. The C4D detector head was immersed in a silicone oil bath (Xiameter PMX200 silicone fluid, 20cS) within the water bath, while the Au sensor microfluidics were immersed directly in the water bath, which was set at 25°C. The reagent bags were not temperature stabilised. A schematic diagram of the experimental setup is shown in Fig. 2.

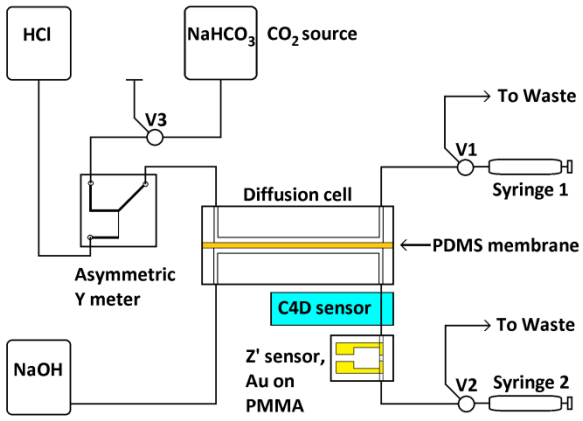

Fig. 2. Schematic diagram of negative pressure system for Z' and C4D measurements of TCO_2. The temperature stabilised water bath is omitted for clarity. The 3-port valves are labelled V1 – V3.

4 Results and Discussion

Optimum test conditions for impedance measurements were initially determined using a KCl salt solution of 141.3 mS m^{-1}. The phase angle reduced to a minimum value at 63096 kHz, for 0.5 mm gap electrodes. The optimum signal to noise ratio (SNR) occurred at an input signal level of 100 mV rms. Continuous impedance measurements were acquired at 0.2 Hz, with a 1s integration time, and the real component Z' recorded. The expected temperature dependence of KCl conductivity is ~ 2% per °C. A 4th order polynomial was fitted to the data to subtract the background drift, and evaluate the residual rms noise, as shown in Fig. 3 (a). The rms noise for the background-subtracted spectrum is 0.61 Ω rms (σ ~ 0.007%) and after a similar drift correction for 9.1 mM (~ 220 mS m^{-1}) NaOH solution, it is 0.39 Ω rms, (σ ~ 0.007%), Fig. 3 (b). The estimated cell constant is ~1140 m^{-1}.

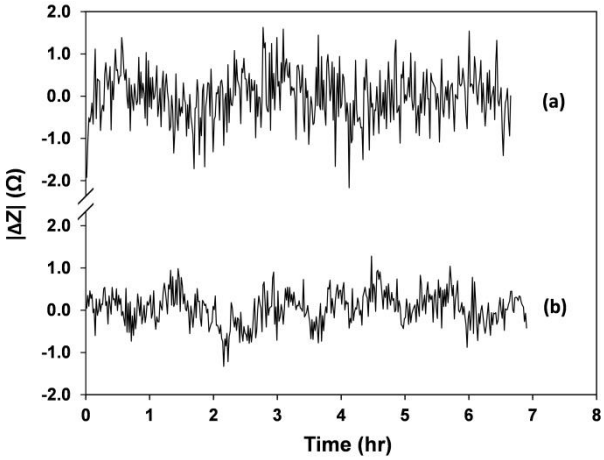

Fig. 3 Time variation in ΔZ' after drift correction, for (a) KCl solution (141.3 mS m^{-1}) and (b) 9.1 mM NaOH solution (~ 220 mS m^{-1}).

The repeatability of the measurement was determined by cyclic switching between two solutions with a nominal conductance difference of 1%. The average ΔZ' was calculated from data sampled, just prior to switching, and the expected noise reduction due to averaging is $N^{1/2}$, where N is the number of samples. A ΔZ' time series (N = 25) is shown in Fig. 4 (63096 Hz, 100 mV rms input, and 0V DC) and the estimated rms noise is ~ 0.05%. This compares with spectrophotometric and conductimetric field precision values (RSD) of 0.14% - 0.18% and indicates that microlitre direct-contact conductivity cells with thin film electrodes can achieve sufficiently low rms noise.[19,21,25]

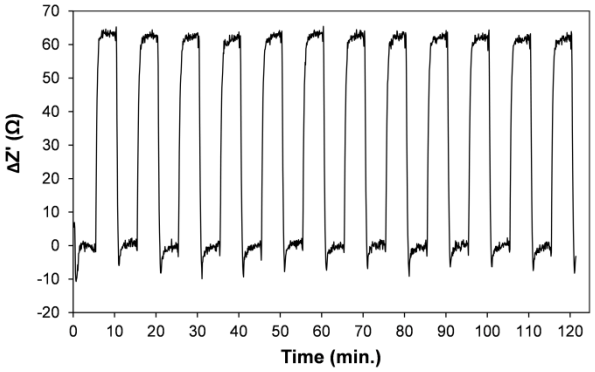

Fig. 4 Repeatability data for switching between two fluids with a conductivity difference of 1% (139.9 mS m^{-1} and 141.3 mS m^{-1})

For TCO_2 calibration testing, under static pre-mix conditions, 200 μL sample and receive chambers were used with a 50 μm PDMS membrane. Diffusion tests were carried out for 2000 μM TCO_2 and 0.5 mm electrode gap, at 100 kHz and 100 mV rms. Each elution peak was ~120 s with peak heights of ~ 6500 Ω, after background subtraction. Although the measured SNR (>900), Fig. 3, indicates a maximum precision of 0.007%, the observed rms variation in Fig. 4 is ~ 0.7%. The calibration curve for 1000 μM – 3000 μM TCO_2 is given in Fig. 5 and is observed to be linear (R^2 > 0.99) over this range. The RSD (not shown) is less than 0.8%. The predicted calibration curve, using a cell constant value of 2100 m^{-1} obtained from 2D finite element simulation for an electrode gap of 0.9 mm is also shown.

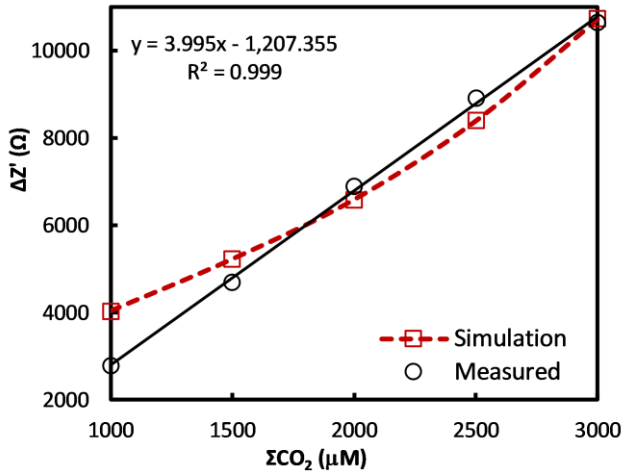

Fig. 5 TCO_2 calibration for 200 µL sample and receive chambers and 20 min diffusion (0.9 mm gap, 100 mV rms, 0V DC, 100 kHz). The theoretical calibration curve (red) is estimated using a cell constant value of 2100, obtained from 2D finite element simulation of the conductivity cell.

Under continuous flow conditions, using acid injection into the DIC loaded flow stream, elution peak sequences were obtained for direct contact (50 kHz, 100 mV rms, 0V DC) and C4D conductivity cells, examples of which are shown in Fig. 6. The elution characteristics were tested for various membrane diffusion periods from 5 min until 45 min and under low and high flow conditions, Fig 7. Measurement precision was determined from peak sequences taken over many hours with peak heights and area values extracted using an automatic procedure. Firstly, a quadratic Savitzky-Golay smoothing function was applied to the raw signal and using the 1st and 2nd Savitzky-Golay derivatives, the start, end and peak positions were obtained, Fig 8.[34] The baseline represents the conductivity of the NaOH blank, the average value of which was determined using a 50 s window on either side of each peak, offset from the peak start and end points by 25 s, and subsequently subtracted from the signal. The ultimate achievable precision values, obtained from baseline SNR, are ~ 0.10% and ~ 0.15%, for Z' and CFD respectively. However, the uncertainty in Z' and C4D signal peak height and area values, obtained from the long sequence measurements, depends on diffusion time and flow rate.

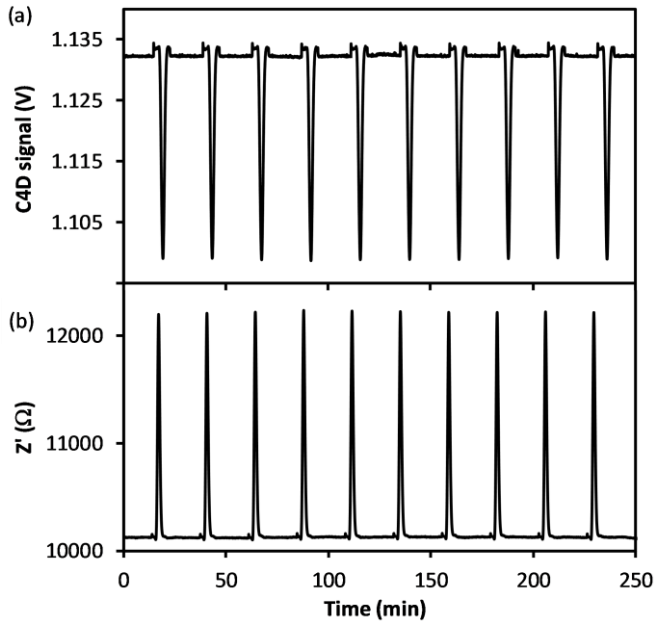

Fig. 6 (a) C4D peak sequence sample with 2000 µM TCO_2 solution, a 100 µL channel and diffusion time of 15 min, **(b)** Z' peak sequence sample under same conditions. The conductivity cell interelectrode gap was 0.9 mm.

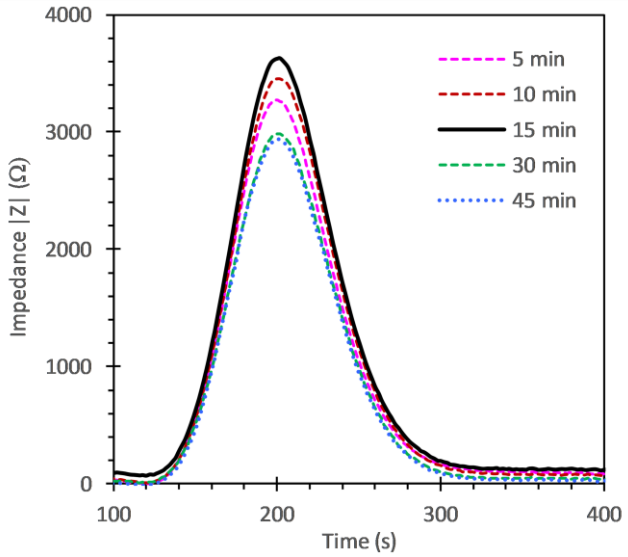

Fig. 7 Elution peak characteristics for diffusion times up to 45 min, with 7 mM NaOH receiving solution.

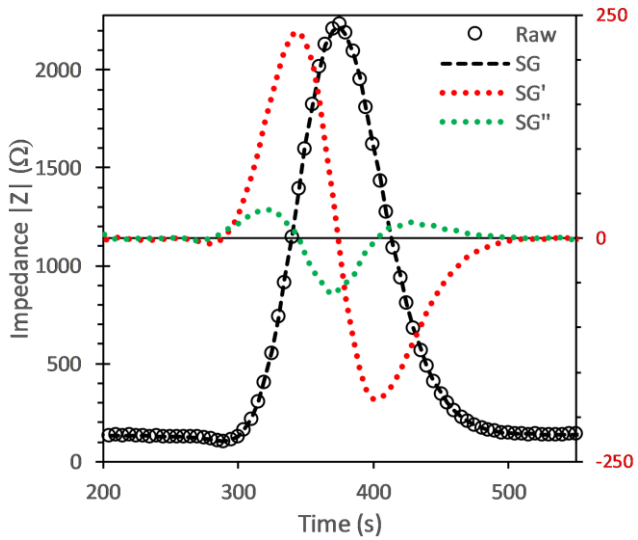

Fig. 8 Elution peak raw data to which a Savitzky-Golay smoothing function is applied (SG). The generated 1st (SG') and 2nd (SG'') derivatives are used to determine start and end points, along with peak position.

The peak height and its RSD variation with diffusion time is shown in Fig. 9. The former increases with diffusion time up to 15 min and then falls thereafter, while the RSD variation is almost the inverse, decreasing to a minimum of < 0.2% for 30 min diffusion. The DIC mass transfer ratio, obtained from integrating the area under curve, follows the same trend as peak height with a maximum value of 80% occurring after 15 min diffusion, falling to ~65% after 45 min. Under low flow conditions, the average pulse width varied from 210 s to 228 s. This equates to a reagent volume of ~350 µl, for a sample input volume of 100 µL. Increasing the flow rate by a factor of 7.5 to 12 µL s^{-1}, results in higher RSD with reduced peak heights and mass transfer ratios of around 70% or less. The reagent volume increased to > 600 µL but the pulse width reduced to ~ 50 s. The equivalent analysis using peak areas rather than heights showed similar trends but the RSD values were higher, with a minimum of 0.5% after 15 min diffusion.

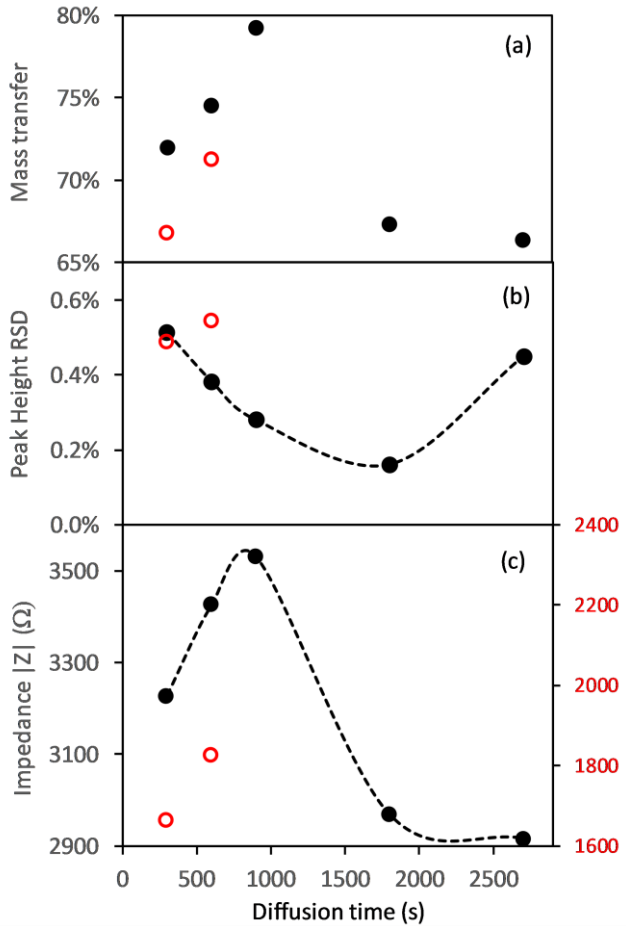

Fig. 9 (a) Mass transfer ratio across membrane against diffusion hold time for low (solid black, 1.6 μL s^{-1}) and high (red, 12 μL s^{-1}) flow conditions. (b) Background-subtracted Z' peak RSD and (c) absolute height values for 2000 μM TCO_2.

There are several potential contributing factors to the observed precision and any given condition. Some will remain intrinsic to the microfluidic device, while others may be influenced by laboratory experimental conditions. The latter include syringe precision, bench electronics and instrumental temperature fluctuation. Ocean capable fixed volume solenoid pumps offer much better precision than bench equivalents. The electronic noise level will depend on the number of useful measurements as $N^{0.5}$, which in turn depends on measurement frequency, CO_2-loaded NaOH volume and flow rate. The dedicated C4D electronics allows sampling rates of up to 100 Hz at a single excitation frequency whereas the Solartron in this set up is limited to a maximum sampling rate to 1.0 Hz. The use of a low flow rate is limited by analyte diffusion, discussed below.

The differences in C4D results here (0.25%) compared to those reported by Bresnahan and Martz (0.1%) for a similar measurement setup, are due primarily to the use of long (165 mm) tubular membranes, in the latter case, with a high surface area to volume ratio. They observed precision values > 0.5% for planar cell constructions but performance improved by increasing sample volume and, to a lesser degree, diffusion time. The latter determines the equilibration fraction. Assuming similar diffusion rates for CO_2 in PDMS and water, the time constant ($l = \sqrt{Dt}$) for filling a 1 mm deep receiver chamber is approximately 500 s and hence the 80% equilibration after a 900 s exchange diffusion time, Fig. 9 is to be expected .[35,36] Complete equilibration therefore requires extended diffusion times or a reduction in the chamber depth. The latter option significantly increases flow resistance and hence the achievable flow rate, for given pump capability and power, and would also limit the depth sampling resolution. While longer diffusion times would increase the analyte concentration in the receiver chamber, sideways diffusion along input and output channels of the receiving chamber will widen the elution peak and increase effective losses as the edge concentrations approach a limit of detection (LOD) around 20 – 25 μmol kg^{-1} (~3σ). Similar diffusion will also occur on the sample side, exacerbating this issue. To avoid the need for additional check valves either side of sample and receive chambers, we investigated the approach of using large chamber volumes with narrow inlet and outlet

channels to minimise mass diffusion. However, increasing the chamber width or depth led to significant analyte trapping in dead zones and required greatly increased sample and reagent volumes for flushing between individual samples. We also observed, especially with wider channels, oscillatory flexing of the membrane into the receive chamber. This may set up pulsating flow or partial blockage and needs to be minimised or avoided altogether. The use of microfluidic volume exchange and conductivity cells demonstrates the feasibility of the proposed approach for long-term chemical analysis. It highlights the possible trade-off between analysis time (equilibration and measurement) and precision. Under ocean conditions the float ascent rate is 0.095 ms^{-1}. At the shortest possible sampling and analysis time of 400 s for the 100 μL cell (10 s sampling, 300 s diffusion, 50 s measurement at high flow), the observed precision is ~0.5%. This would equate to a DIC resolution (3σ) of ~30 μmol kg^{-1}, for samples collected every 38 m with a maximum depth resolution of 1 m. A full profile would therefore collect ~50 sample datasets and over the life of the float (~120 profiles) would require a minimum of ~ 4 L of NaOH and 0.1 L of HCl. Alternatively, since the Argo float is parked at depth between profiles for ~10 days, it may be preferred to collect samples during descent (depth resolution 0.4 m) and use extended analysis times for improved precision. While this, in theory, would allow for > 200 samples per profile, storage volume and power constraints would reduce this number considerably. With 100 samples per profile, the reagent payload would be ~ 5L and to reduce this to a likely volume storage limit of 1 L will require commensurate reduction of the exchange and conductivity cell volumes without loss of precision. To avoid inter-sample diffusion over the extended analysis period will require development of robust ultra-small non-hydraulic microvalve networks.

5 Conclusions

Conductimetric determination of dissolved inorganic carbon concentration, in the seawater range of 1000 – 3000 μmol kg^{-1}, has been achieved using a microfluidic thin film electrode conductivity cell and a membrane-based gas exchange cell. After transfer across the membrane, the eluted CO_2 reacted in a NaOH carrier, was drawn through a conductivity cell, with a < 1 μL interelectrode volume, where the change in impedance versus time was measured. Minimum precision values obtained from relative standard deviation were ~ 0.2 % from peak height and 0.5% from area under curve. This compares favourably with precision values of ~ 0.25 % obtained using a large C4D electrophoresis headstage of similar active measurement volume. The required sample and reagent volumes amounted to ~ 500 μL in total due to the incorporation of a planar membrane into a small volume exchange cell. This compares very favourably with previous attempts at conductivity based DIC analysis where total volumes between 5000 μL and 10000 μL were required while achieving precision values approaching 0.1% also necessitated the use of 20 cm long membrane tubes and wire electrodes. The achievement here of high accuracy miniaturisation demonstrates the feasibility of developing a lab on chip based conductimetric analysis approach for autonomous and long-term continuous measurement of ocean chemistry via float deployment. Performance improvement in the near future will require addressing membrane chemical and mechanical stability as well as volume reduction and component integration into a single manifold.

Acknowledgements

The authors would like to acknowledge the funding support from Invest N. Ireland (RD0714186), the Department of Employment and Learning, N. Ireland (US-IRL 013), Science Foundation Ireland (09/US/I1758), and National Science Foundation (US) (NSF 0961250). We would also like to acknowledge Todd Martz and Phil Bresnahan of Scripps Institute of Oceanography, UC San Diego.

Conflict of Interest.

The authors declare that they have no conflict of interest.

References

1 C. L. Sabine, R. A. Feely, N. Gruber, R. M. Key, K. Lee, J. L. Bullister, R. Wanninkhof, C. S. Wong, D. W. R. Wallace, B. Tilbrook, F. J. Millero, T. -. Peng, A. Kozyr, T. Ono and A. F. Rios, *Science*, 2004, **305**, 367-371 (DOI:10.1126/science.1097403).
2 F. J. Millero, *Chem. Rev.*, 2007, **107**, 308-341 (DOI:10.1021/cr0503557).
3 Surface Ocean CO2 Atlas (SOCAT), www.socat.info, (2016).
4 V. M. C. Rérolle, E. P. Achterberg, M. Ribas-Ribas, V. Kitidis, I. Brown, D. C. E. Bakker, G. A. Lee and M. C. Mowlem, *Sensors*, 2018, **18**, 2622 (DOI:10.3390/s18082622).
5 J. S. Clarke, M. P. Humphreys, E. Tynan, V. Kitidis, I. Brown, M. Mowlem and E. P. Achterberg, *Frontiers in Marine Science*, 2017, **4**, 396 (DOI:10.3389/fmars.2017.00396).
6 R. H. Byrne, *Environ. Sci. Technol.*, 2014, **48**, 5352-5360 (DOI:10.1021/es405819p).
7 T. Hansen, B. Gardeler and B. Matthiessen, *Biogeosciences*, 2013, **10**, 6601-6608.

8 P. D. Tortell, *Limnology and Oceanography: Methods*, 2005, **3**, 24-37.
9 C. Guéguen and P. D. Tortell, *Marine Chemistry*, 2008, **108**, 184-194.
10 R. J. Bell, R. T. Short and R. H. Byrne, *Limnol. Oceanogr. Methods*, 2011, **9**, 164-175 (DOI:10.4319/lom.2011.9.164).
11 L. Freije-Carrelo, L. Alonso Sobrado, M. Moldovan, J. R. Encinar and J. I. García Alonso, *Anal. Chem.*, 2018, **90**, 4677-4685 (DOI:10.1021/acs.analchem.7b05242).
12 S. Kaltin, C. Haraldsson and L. G. Anderson, *Marine Chemistry*, 2005, **96**, 53-60.
13 A. J. Fassbender, C. L. Sabine, N. Lawrence-Slavas, E. H. De Carlo, C. Meinig and S. Maenner Jones, *Environ. Sci. Technol.*, 2015, **49**, 3628-3635 (DOI:10.1021/es5047183).
14 A. M. Bass, M. I. Bird, M. J. Morrison and J. Gordon, *Limnology and Oceanography: Methods*, 2012, **10**, 10-19.
15 A. M. Bass, M. I. Bird, N. C. Munksgaard and C. M. Wurster, *Rapid Commun. Mass Spectrom.*, 2012, **26**, 639-644 (DOI:10.1002/rcm.6143).
16 M. D. DeGrandpre, T. R. Hammar, S. P. Smith and F. L. Sayles, *Limnol. Oceanogr.*, 1995, **40**, 969-975 (DOI:10.4319/lo.1995.40.5.0969).
17 Y. Nakano, H. Kimoto, S. Watanabe, K. Harada and Y. W. Watanabe, *J. Oceanogr.*, 2006, **62**, 71 81 (DOI:10.1007/s10872-006-0033-y).
18 Z. A. Wang, X. Liu, R. H. Byrne, R. Wanninkhof, R. E. Bernstein, E. A. Kaltenbacher and J. Patten, *Analytica Chimica Acta*, 2007, **596**, 23-36 (DOI:https://doi.org/10.1016/j.aca.2007.05.048).
19 Z. A. Wang, S. N. Chu and K. A. Hoering, *Environ. Sci. Technol.*, 2013, **47**, 7840-7847 (DOI:10.1021/es400567k).
20 X. Liu, R. H. Byrne, L. Adornato, K. K. Yates, E. Kaltenbacher, X. Ding and B. Yang, *Environ. Sci. Technol.*, 2013, **47**, 11106-11114 (DOI:10.1021/es4014807).
21 Z. A. Wang, F. N. Sonnichsen, A. M. Bradley, K. A. Hoering, T. M. Lanagan, S. N. Chu, T. R. Hammar and R. Camilli, *Environ. Sci. Technol.*, 2015, **49**, 4441-4449 (DOI:10.1021/es504893n).
22 A. G. Dickson, C. L. Sabine and J. R. Christian, *Guide to best practices for ocean CO2 measurements. PICES Special Publication 3*, North Pacific Marine Science Organization, Canada, 2007.
23 P. Hall and R. Aller, *Limnol. Oceanogr.*, 1992, **37**, 1113-1119 (DOI:10.4319/lo.1992.37.5.1113).
24 Earth System Research Laboratory: Global Monitoring Division, https://www.esrl.noaa.gov/gmd/ccgg/data-products.html, (accessed 06/17 2019).
25 F. L. Sayles and C. Eck, *Deep-Sea Res. Part I Oceanogr. Res. Pap.*, 2009, **56**, 1590-1603 (DOI:10.1016/j.dsr.2009.04.006).
26 P. J. Bresnahan and T. R. Martz, *IEEE Sensors Journal*, 2018, **18**, 2211-2217 (DOI:10.1109/JSEN.2018.2794882).
27 J. N. Plant, K. S. Johnson, J. A. Needoba and L. J. Coletti, *Limnol. Oceanogr. Methods*, 2009, **7**, 144-156 (DOI:10.4319/lom.2009.7.144).
28 C. Henríquez, B. Horstkotte and V. Cerdà, *Talanta*, 2014, **118**, 186-194 (DOI:https://doi.org/10.1016/j.talanta.2013.10.005).
29 Z. Hoherčáková and F. Opekar, *Analytica Chimica Acta*, 2005, **551**, 132-136 (DOI:https://doi.org/10.1016/j.aca.2005.07.029).
30 P. Bresnahan, T. Martz, J. deAlmeida, B. Ward and P. D. Maguire, *Oceanography*, 2017, **30**, 32 (DOI:10.5670/oceanog.2017.215).
31 , http://www.argo.ucsd.edu/, (accessed 7/18/2016 2016).
32 M. Tweedie, D. Sun, B. Ward and P. D. Maguire, *Lab Chip*, 2019, **19**, 1287-1295 (DOI:10.1039/C9LC00123A).
33 D. Sun, M. Tweedie, D. R. Gajula, B. Ward and P. D. Maguire, *Microfluid. Nanofluid.*, 2015, **19**, 913-922 (DOI:10.1007/s10404-015-1620-2).
34 P. A. Gorry, *Anal. Chem.*, 1991, **63**, 534-536 (DOI:10.1021/ac00005a031).
35 T. C. Merkel, V. I. Bondar, K. Nagai, B. D. Freeman and I. Pinnau, *Journal of Polymer Science: Part B: Polymer Physics*, 2000, **38**, 415-434.
36 S. P. Cadogan, G. C. Maitland and J. P. M. Trusler, *J. Chem. Eng. Data*, 2014, **59**, 519-525 (DOI:10.1021/je401008s).